Chapter 5

Application of Acoustic Emission Technique in the Monitoring of Masonry Structures

Jie Xu, Qinghua Han and Ying Xu

Additional information is available at the end of the chapter

http://dx.doi.org/10.5772/63093

Abstract

The application of acoustic emission (AE) technique in monitoring the safe condition is a useful technique in steel and concrete structures, whereas its application is restrained in masonry structures due to the layered property. Qualitative and quantitative analyses were investigated in this research to improve the AE application in masonry structures. For quantitative analysis, an improved localization method is proposed to give more reliable crack localization results. In the proposed method, the parameter ξ on the behavior of inhomogeneity of the monitored structure could minimize the unavoidable propagation delay caused by the layers in the masonry structure. The rest results approved the reliability of the proposed method in masonry structures. For qualitative analysis, the parameter analysis, including the cumulative AE event, frequency distribution, time-scaling exponent, and *b*-value, was adopted to monitor one historical church and was approved to be useful.

Keywords: acoustic emission, masonry structures, quantitative analysis, qualitative analysis, crack localization

1. Introduction

Acoustic emission (AE) is the class of phenomena whereby transient elastic waves are generated by the rapid release of energy from a localized source or sources within a material. Clearly, an AE is a stress wave that travels through a material as the result of some sudden release of strain energy. By investigating their origin and characteristics, AE techniques provide an insight into the deterioration processes of a tested object, especially for the monitoring and nondestructive testing of the structural integrity and general quality.

Significant research work has been published in relation to the use of AE sensors for monitoring the health of structures in civil engineering, especially for concrete structures. The most important applications of AE to concrete elements started in the late 1970s, when the original technology developed for metals was modified to suit heterogeneous materials [1,2]. Some fundamental studies with small-scale specimens have shown that, in principle, AE analysis is an effective method for damage assessment [3]. Research from various laboratory loading tests to full-scale models of real structural components was intended to relate observed AE characteristics to failure mechanisms in reinforced or prestressed concrete [4–7]. Some applications were tried to evaluate the structural integrity, load-carrying capacity, or eventual failure for real civil engineering structures such as concrete bridges and so on [8]. Also, a continuous monitoring of a whole structure is applicable (e.g. to detect wire breaks of prestressing tendons) [9]. The development of the corresponding AE equipment, such as wireless monitoring system with microelectromechanical system (MEMS) sensors [10], also furthers the AE research.

As AE gained importance for concrete structures, its application for masonry structures is gradually employed [11]. Huge numbers of ancient masonry structures, such as towers and bridges, are present all over of the world. To preserve this inestimable cultural heritage, a sound safety assessment should taken into account the evolution of damage phenomena [12]. In this respect, the AE monitoring technique can be highly effective. Some researchers [13] have successfully applied AE techniques to monitor masonry buildings, towers, and bridges. In these researches, the interpretation of AE rate has been put forward to monitor the criticality of the ongoing process, and the "*b*-value" analysis was used and proven as a useful method to determine the propagation of the cracks. Also, an ad hoc theory based on fractal concepts for assessing the stability of masonry structures from the data obtained with the AE technique is proposed. In the application [14], a series of multiring brickwork arches have been tested to assess the applicability of the AE technique for masonry arch bridges under static and long-term cyclic loading to study crack propagation and failure mechanisms. A series of short-term creep tests and compressive tests were performed on masonry columns by Verstrynge et al. [15], and they found that the damage accumulation parameter, calculated from the AE results, shows a linear increase in the function of the relative stress level.

However, unlike the conditions in concrete, AE applications in masonry are still at an early stage. The reason is that AE is applicable for homogeneous or quasi-homogeneous materials (e.g. metallic and concrete) with good acoustic transmission. However, its application on heterogeneous materials, such as masonry, is much more problematic, especially in the crack source localization problem. Attempts were made by Carpinteri et al. [16] by involving the location of cracks during an on-site monitoring campaign. Although a large amount of AE events were detected, only a small percentage of them could be located. Damage location in masonry arch bridges was performed by Tomor and Melbourne [17] by simply applying a large set of AE sensors and identifying the sensors at which most damage was detected.

This paper focuses on the applicability of AE technique in the monitoring of masonry structures based on quantitative and qualitative analyses. To address these issues regarding the heterogeneous problem, a series of pencil-lead break tests were carried out on a masonry

http://dx.doi.org/10.5772/63093

bridge and a historical church was monitored by the AE technique. The results are discussed in this chapter.

2. Quantitative analysis

Quantitative analysis is also called the signal-based AE technique, and the time series of AE events are recorded along with their waveforms. Quantitative methods allow a more accurate characterization of the fracture process and try to describe the nature of a source using special methods, such as localization and moment tensor analysis. The goal of quantitative AE analysis is to enumerate and explain the source of an AE event. The principle is that AE burst signals within a given time window are detected by more than one sensor and grouped to an AE event that can be associated with an AE source. Source localization method is one of the important ones adopted in this method.

The crack localization of AE sources is important to evaluate the areas of active damage in the monitored structures. The localization issue is normally solved by triangulation methods based on acoustic signal trajectories [18]. Usually, these methods rely on the elasticity modulus, the propagation mode, and signal attenuation caused by the heterogeneity and anisotropy of the material. In this part, the classical localization method was summarized briefly.

2.1. Classical localization method

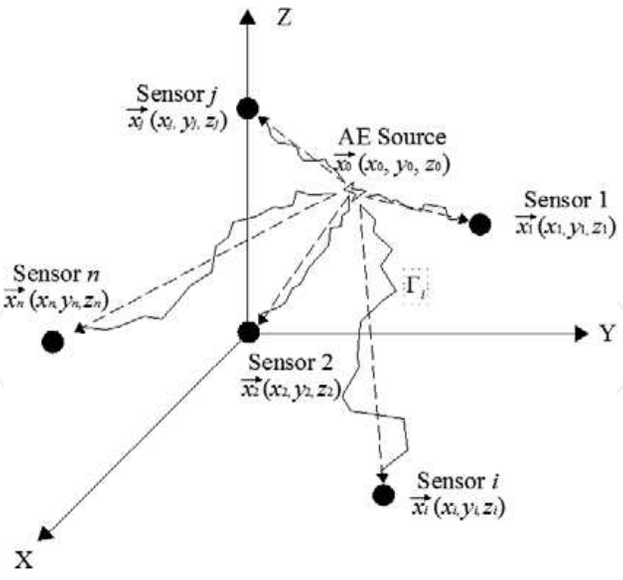

Figure 1. AE source localization by an array of n sensors.

In a theoretical model, with wave propagation velocity v_{Pi}, the arrival time t_i^* at $\vec{x}_i$, unknown coordinates $\vec{x}_0$, and origin crack happening time t_0 can be calculated by an integral along the real path Γ_i, as shown in **Figure 1**:

$$t_i^* = t_0 + \underbrace{\int_{\Gamma_i} (d\Gamma_i / v_{Pi}(r))}_{\mathrm{I}}, \tag{1}$$

where $v_{Pi}(r)$ is the field of wave velocity in the monitored structures. If the material is homogeneous, Equation (1) can be simplified as

$$t_i^* = t_0 + \frac{|\vec{x}_0 - \vec{x}_i|}{v_p} = t_0 + \frac{\vec{x}_{i0}}{v_p}. \tag{2}$$

For each sensor i, there will be residual r_i between the observed arrival time t_i and the calculated arrival time t_i^*:

$$r_i = t_i - t_i^*. \tag{3}$$

If t_j is the arrival time at another sensor $\vec{x}_j$, the detected arrival time difference between sensors i and j is adopted. Usually, we have

$$r_i^* = \Delta t_{i1} - \frac{\vec{x}_0 - \vec{x}_i}{v_p} \left(i = 2, \ ..., n\right), \tag{4}$$

where subscript 1 is related to an arbitrarily chosen reference sensor (e.g. the closest one to the crack source).

If more than four arrival times are available for one event, the equation will be overdetermined. The least-squares method are adopted to minimize the residuals, where the error for (n-1) equations is only the sum of all squared time residuals:

$$\chi^2 = \sum_{i=2}^{n} (r_i^*)^2. \tag{5}$$

Considering Equation (5) is linear, and the issue can be solved iteratively until convergence [19].

2.2. Velocity field of AE-$v_{Pi}(r)$

As shown in Equation (1), the acoustic wave velocity field $v_{Pi}(r)$ is an important point in the calculation. The variation of velocity field $v_{Pi}(r)$ is affected mainly by the material property of

http://dx.doi.org/10.5772/63093

monitored structures. If the structure is homogeneous, the wave propagation path from the crack point to the sensor is surely treated to be a straight one, shown in **Figure 2** by dashed line, and the velocity field $v_{Pi}(r)$ is also homogeneous. Thus, the velocity in the structure is a certain value in every path direction, and v_P can be calculated by Equation (5). The metal material is the typical one that can be considered as homogeneous, and Equation (2) can be applied well for it.

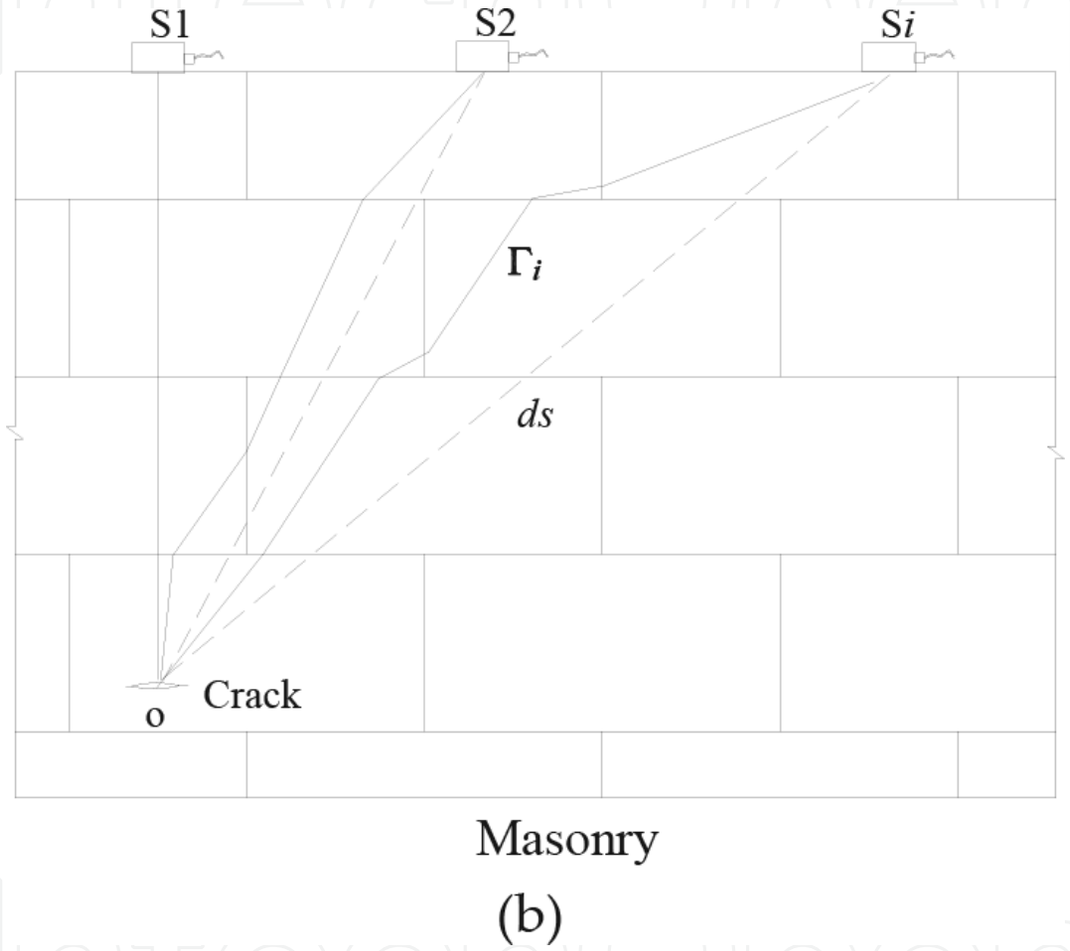

Figure 2. Differences between theoretical wave propagation path and the real path in masonry.

The refraction and reflection of the wave at the layers is unavoidable for masonry materials. Because the reflection phenomenon mainly leads to the decrease of the signal amplitude and of incident energy density, we only take propagation effects related to the refraction of AE wave into consideration. From **Figure 2**, the propagation delays (denoted as *P-D*) are

$$P-D=\frac{\Gamma_i}{v_\Gamma}-\frac{ds}{v_{ds}}=\frac{\int_{\Gamma_i} kdl}{v_{ds}}-\frac{ds}{v_{ds}} \tag{6}$$

where $k = \frac{v_{ds}}{v_\Gamma}$ and v_Γ are the propagation velocity along the real path Γ and v_{ds} is the counterpart along the theoretical path *ds*. Thus, we have

$$P - D = \underbrace{\frac{\int_{\Gamma_i} kdl}{v_{ds}} - \frac{\int_{\Gamma_i} dl}{v_{ds}}}_{Velocity-delay} + \underbrace{\frac{\int_{\Gamma_i} dl}{v_{ds}} - \frac{ds}{v_{ds}}}_{Geometrical-delay} \tag{7}$$

Normally, the difference of velocity in the two different paths for one sensor event is not so obvious and $k = 1.0$. In this case, only the effect of the geometrical delay is considered:

$$P - D = \frac{\int_{\Gamma_i} dl}{v_{ds}} - \frac{ds}{v_{ds}} \tag{8}$$

Generally, the *P-D* value reflects the deviation of the calculated path *ds* from the real wave propagation path Γ_i between the crack point and the sensor. The *P-D* value will increase as the traveling path increases, because the practical situations will be more complicated for propagating through more layers. In this point, the *P-D* value surely exists in masonry structures, which means that the traditional method based on Equation (2) cannot be used here directly.

2.3. Test set-up and velocity field modification

Several pencil-lead break tests based on a two-arch masonry bridge model are conducted in this research to improve the source localization problem in the masonry structure.

2.3.1. Monitoring system of AE

The AE monitoring set-up consisted of six piezoelectric (PZT) sensors and six control units and a PC-based multichannel monitoring system called SAMOS AEwin (Sensor-based Acoustic Multichannel Operating System) that is manufactured by Physical Acoustic Corporation (PAC). Appropriate AE sensor types are important in the fracture monitoring of concrete structures. Because concrete is known to be a highly attenuating material, lower-frequency sensors are suitable for AE studies. The maximum aggregate size in concrete for the present study is 20 mm, and 3500 m/s is normally used as sound velocity in concrete. Using the relation $V=n\lambda$, the frequency of the AE sensor to be used is desirable to be less than 180 kHz, and this frequency is within the range of 100 to 500 kHz. Considering this point, another R15A with highest sensitivity between 50 and 400 kHz (**Figure 3a**) was selected in the test. The gains of the preamplifiers and the acquisition system were set to 20 and 40 dB, respectively. The acquisition threshold was set to 40 dB to ensure a high signal-to-noise ratio to avoid back-

http://dx.doi.org/10.5772/63093

ground noise. Vacuum grease LR (high vacuum silicon grease) was used as a coupling agent to fix the sensors on the opposite surfaces of the concrete. The band-pass analog filter is set to between 20 kHz and 2 MHz, and the sampling frequency is set to 10 MHz.

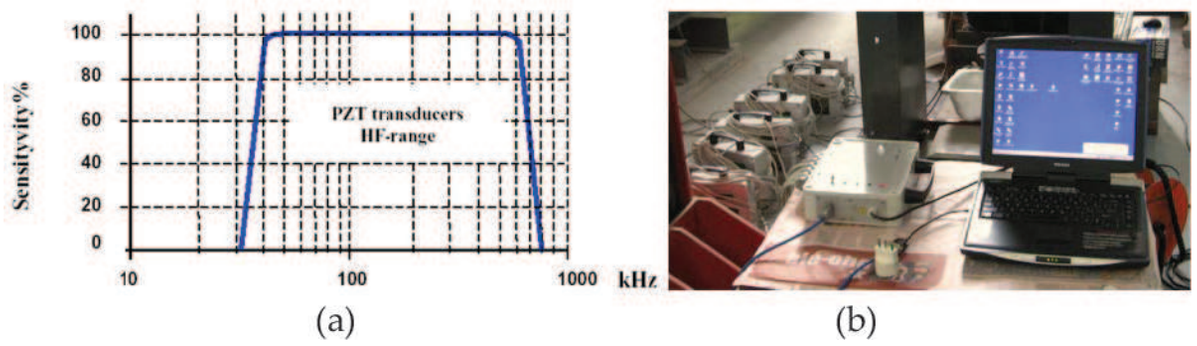

Figure 3. (a) AE sensor frequency bands and (b) acquisition system of AE system.

2.3.2. Bridge model and material property

A two-arch masonry bridge model was designed and the scale of the bridge model is 1:2 and it is 5.90 m long, 1.60 m wide, and 1.75 m high according to the theory of models. Bricks with a uniform size of 130×65×30 mm were made by hand. The mechanical properties of masonry brick and mortar were selected to better represent the real historical bridges. The bridge has two masonry abutments and a central pier. The abutments set on basements are built by concrete and anchored to the ground with special reinforcements, as shown in **Figure 4**. The details of the bridge can be found in our previous paper.

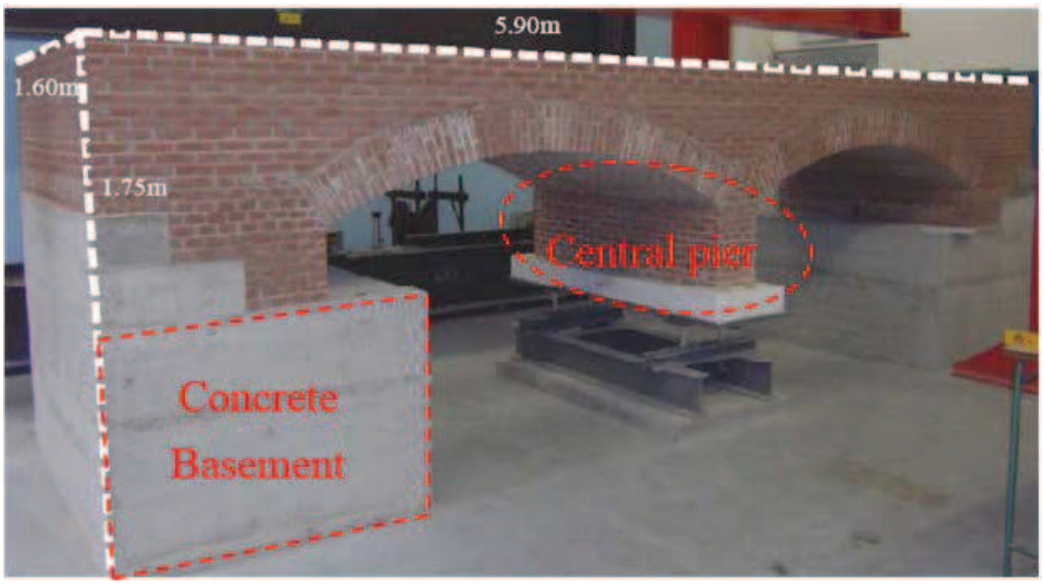

Figure 4. Bridge model and its dimension.

Before the tests, it is necessary to evaluate the mechanical properties of the bridge, such as the basic material (i.e. the masonry).

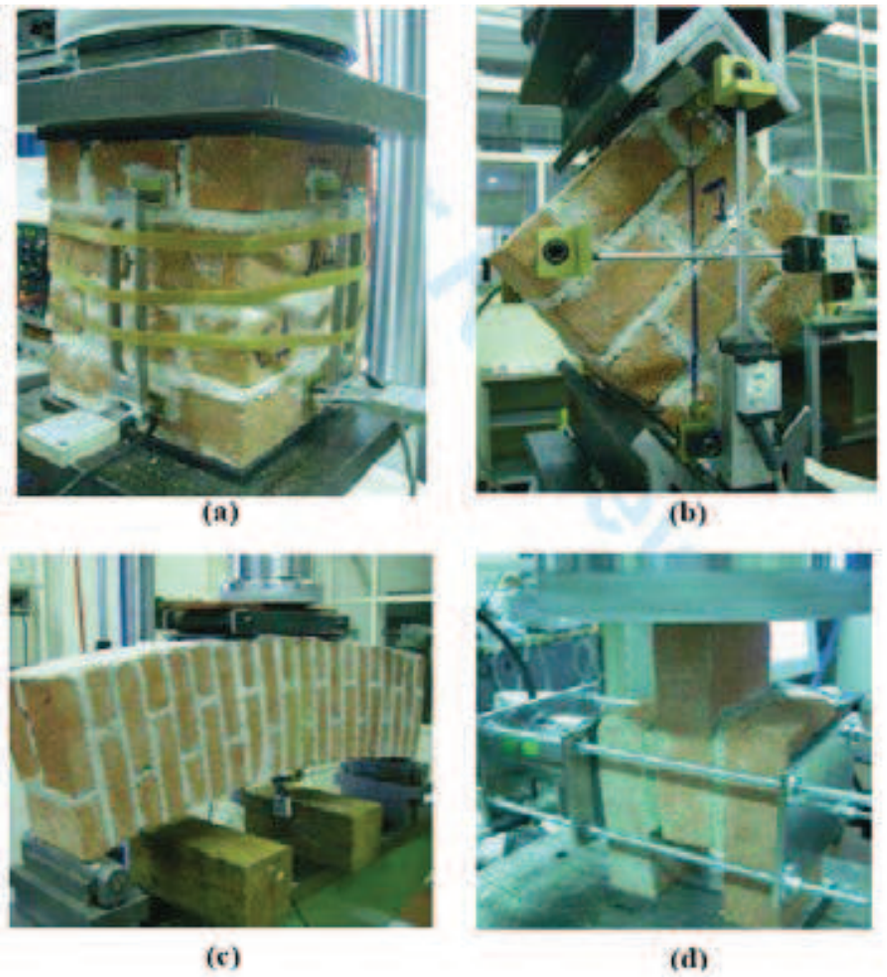

Figure 5. Mechanical tests for the masonry: (a) compression, (b) diagonal compression, (c) four-point bending test of arch, and (d) shear test.

As shown in **Figure 5**, different kinds of laboratory tests have been conducted to estimate the mechanical parameters of the bridge. Besides, tests about the mortar itself and on the concrete to support the abutments were also performed. The key mechanical parameters extracted are the Young's modulus E, tensile strength f_t, Poisson ratio v, tensile fracture energy G_F, and compressive strength f_c. The detailed information about the parameters related to our research can be found in **Table 1**.

Parameter	γ **[kg/m³]**	E **[Pa]**	ν -	f_c **[Pa]**	f_t **[Pa]**	G_F **[Nm]**
Value	1900	1.5×10^9	0.2	3×10^5	4.3×10^6	400

Table 1. Mechanical parameters of materials extracted from the tests.

http://dx.doi.org/10.5772/63093

2.3.3. Tests of velocity field

Figure 6. Wave velocity test: (left) the sketch of the pencil-lead break point and the sensor distribution and (right) scenario of the velocity test.

As shown in **Figure 6**, sensors (S_0-S_5) are adopted to monitor acoustic data, and the distance between two neighbored sensors increases from S_0-S_1 to S_4-S_5 with an increment value of 5 cm. During the test, the pencil was broken beneath the S_0 sensor, 5 cm away from the same surface, to analyze velocity propagation in the surface, as shown in **Figure 6**. At the same time, AE wave propagation inside the masonry bridge was also investigated through the same sensor array shown in **Figure 6**, and the pencil was broken on the opposite surface of the central pier but at the same corresponding position of sensor S_0.

The test results of the detected velocities are shown in Figures 7 and 8. The labeled velocity *V*-homogeneous is calculated based on the mechanical properties in Table 1 for comparison. The labeled velocity *V*-average is the average value of all the calculated velocities from the corresponding test.

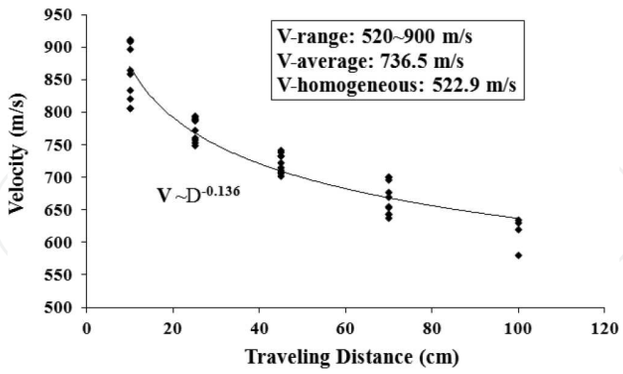

Figure 7. AE velocity on the masonry surface of the bridge model.

In **Figures 7** and **8**, the velocities, both on surface and inside the masonry, show that the velocity decreases clearly with the increasing propagating distance. The explanation is that the transient wave changes its mode from longitudinal to shear and/or to surface waves and vice versa due to the refraction and/or reflection during propagation in different phases. The longer the propagating distance is, the more mode change happens, which causes a bigger deviation

of the actual wave propagation path Γ_i from the calculated one *ds*. This is just what we named the phenomenon of propagation delay in Equation (8).

From **Figures 7** and **8**, we can see that there is a great difference between the *V*-homogeneous and the *V*-average, so we cannot take the masonry as a homogeneous material in initial guess. In this case, the *V*-average from the field velocity test is used as the value in the initial guess to start the iteration of calculation for the source localization.

2.3.4. Modified source localization method in masonry

Based on the classical method, a modified method is proposed in this part. The basic idea of the source localization in masonry material is similar as that in concrete. However, modifications for propagation delay are implemented. We still take the geometry distance *ds* as the calculated path, as it is not possible to know the actual wave path Γ. However, time-delay modification can be made according to the velocity properties in **Figures 7** and **8** to reduce the effect of inhomogeneous property. In the proposed modified model, the classical model result in Equation (5) is modified into

$$\chi^2 = \sum_{i=2}^{n} (r_{i1})^2 = \sum_{i=2}^{n} \left[x_{10} - x_{i0} - (k_i t_i - t_1) v_1 \right]^2, \tag{9}$$

where $k_i = (d_1 / d_i)^{\xi}$ is the modified factor used to modify the effects of propagation delay or the inhomogeneity. The parameter ξ, named as degree of the inhomogeneity, in k_i reflects the inhomogeneous degree of the material. The ξ is calculated from the pencil-lead break wave velocity filed test result, as shown in **Figure 7**. It shows the relation between the wave propagation distance and the calculated velocity. In ideal homogeneous materials, the value ξ is 0 because the wave velocity is a constant value with change of traveling distance. However, the value ξ will increase with the degree of the heterogeneity if the material is not homogeneous. In our research, the degree of the inhomogeneity ξ is 0.14 as calculated from the

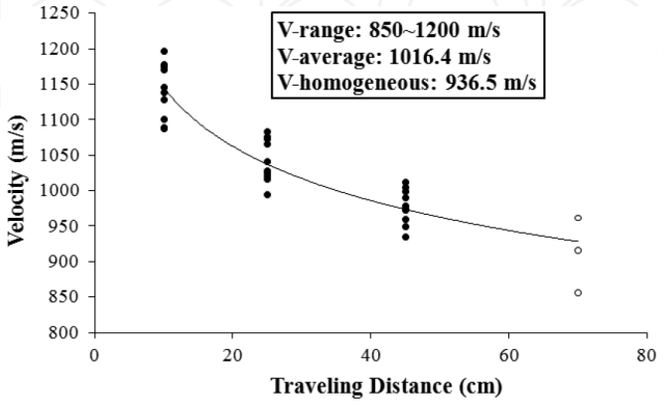

Figure 8. AE velocity inside the masonry model bridge.

http://dx.doi.org/10.5772/63093

relationship between the traveling distance and the velocity, as shown in **Figure 7**. The procedure to determine the crack source by the modified localization method is shown in **Figure 9**.

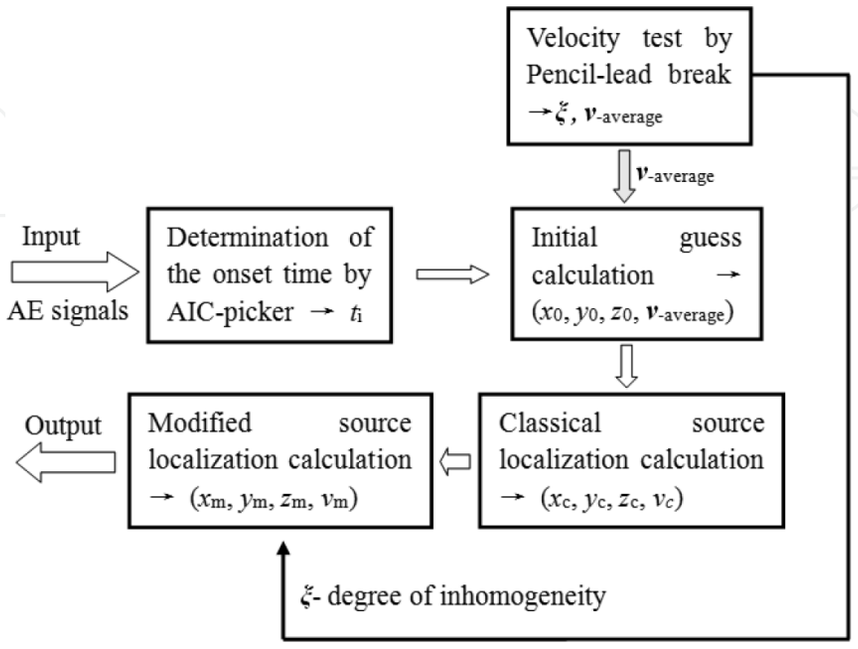

Figure 9. Flow chart of the proposed source localization method.

2.3.5. Validation of the modified localization methods

Pencil-lead break tests are conducted to produce AE source on the right-side surface of the masonry bridge. As shown in **Figure 10**, six sensors described in Section 2.3.1 are attached to the surfaces. Nineteen different points were selected to make a pencil-lead break (artificial

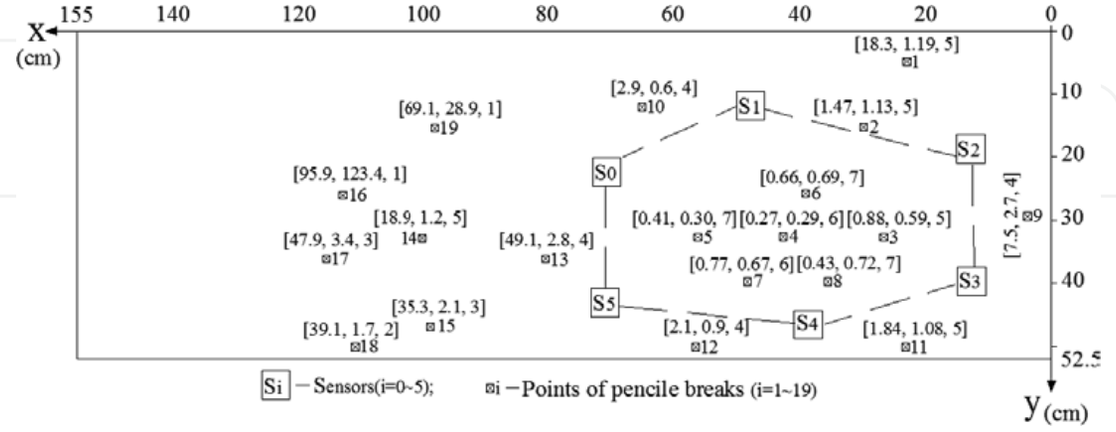

Figure 10. Crack source localization results from the traditional and the proposed modified methods. For [*a, b, c*], *a* is the average error from the traditional method, *b* is the average error from the modified method, and *c* is the source breaks used for each point.

source), and a pencil was broken eight times for each point, so totally 152 signal results are recorded. Nine hundred twelve AE events were obtained from the six sensors in this test and then all the 19 points were source localized following the procedure shown in **Figure 9**.

The localization results are shown in **Figure 10** for both the proposed modified and traditional methods. It is clearly shown that the location accuracy changes with the source break position. According to the accuracy, we divided the break points into three groups. As the dashed line shown in **Figure 10**, points 3 to 8 inside the central area of the sensor network have the best accuracy for localization for both methods. In the second group, points 2, 9, 10, 11, and 12, distributed on the nearby region of the sensor network, comprise the second group. Points in the third group are the rest of the points, far from the sensor network.

In the first group, the two methods both get the ideal result, the errors are all smaller than 6 mm, and most crack sources can be detected. In the second group, the proposed modified model gives better localized results than the traditional method. The errors value (*a* in **Figure 10**) in the traditional method is 15 to 75 mm, whereas the errors value (*b* in **Figure 10**) can be reduced to 6 to 27 mm in the proposed modified method. In this group, about half of the break sources can be monitored based on the value *c* in **Figure 10**. The result from the traditional method for the third group is hardly acceptable for its huge errors, but the proposed modified method can be still in good results. Although the errors are 3 or 4 cm, which are slightly large, the localized results are still acceptable if compared to the total size scale of the surface.

From the test results, compared to the traditional method, the proposed modified method can give better source localization results for the masonry structure in all the three group conditions.

3. Qualitative analysis

Qualitative analysis, also called the parameter-based AE technique, extracts only parameters but the signal itself. The parameters usually used are arrival time, amplitude, duration, number of oscillations, and so on. The typical methods employed in the parameter-based technique are ring-down counting and event counting, in which the event intensity is measured by the oscillation number NT, and the oscillation number NT increases with the signal amplitude.

To express the application of qualitative analysis, we applied the AE technique to monitoring one historical chapel, which is located in north Italy of Sacro Monte di Varallo. In this monitoring, our task is to investigate the stability of the painted plaster walls and injuries with the technical AE. The monitoring structure is the Chapel XVII of the Sacred Mountain of Varallo. The cumulative AE event, frequency distribution, time-scaling exponent, and *b*-value were adopted in this monitoring for the qualitative analysis.

3.1. Scenario of the monitored heritage chapel

The Sacred Mountain of Varallo is one of the oldest Italian constructions in its style. It was constructed in 1491 by San Francesco. The Sacro Monte was built on a rocky foundation, located

http://dx.doi.org/10.5772/63093

on the slopes of Mount of Three Crosses, and River Sesia is on the left side. This natural formed terrace (600 m) soars up the historic center of Varallo (450 m) about 150 m.

The Sacred Mountain of Varallo consists of a basilica and 45 chapels, either isolated or inserted into the large monumental complexes, famous by more than 800 life-size painted statues, in wood and terracotta, which dramatically illustrate the life, passion, death, and resurrection of Christ. These interiors are vividly decorated with fresco paintings. **Figure 11** is a point view of Sacro Monte.

Figure 11. Overall view of the square of the courts.

Figure 12. Out view of the Chapel XVII.

The first monitored structure by AE technique was chosen as the Chapel XVII, which tells the story of the transfiguration of Christ on Mount Tabor, as shown in **Figure 12**. Chapel XVII was constructed starting from the foundations in 1572 but was finished only in the 1760s.

As shown in **Figure 13a**, the frescoes inside the Chapel XVII are the outcome of the brothers Montaldo, who also are the makers of the decoration of the dome of the Basilica of the Sacred Mountain. The statues attributed to Peter and John Francis Petera Varallo Camasco by Soldo were finished in the 1770s, as shown in **Figure 13b**.

Figure 13. Inside view of the Chapel XVII: (a) the frescoes and (b) the status of the Peter and John Francis Petera.

3.2. In-site monitoring by AE technique

The target is to set the sensors for the monitoring of AE signals from a lesion in the north wall of the chapel and a detachment of the fresco. On the other hand, some of the terracotta statues in the chapel were also analyzed (**Figure 14**).

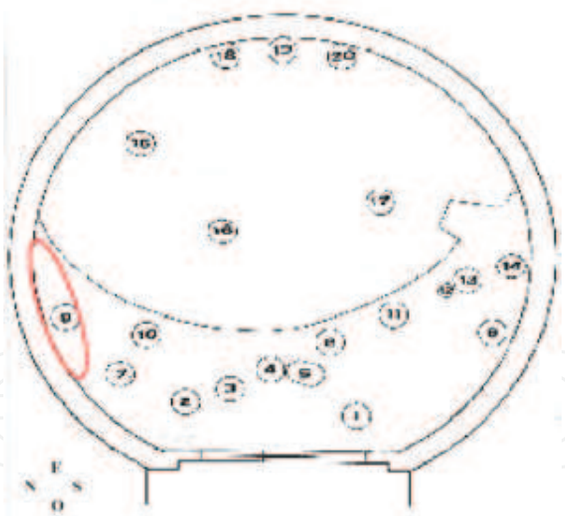

Figure 14. Top-to-down view of the Chapel XVII. The monitoring region is inside the red line.

Some necessary previous operations were carried out by professional restorers for attaching the AE sensors on the wall. First, areas were selected and prepared for monitoring with the films of Japanese paper, of which the surface was then stretched out a hand of light "Paraloid", as shown in **Figure 15a**. This is one kind of acrylic resin that is used in restoration as a consolidation at low concentrations (2–4%) or glue at higher concentrations. As shown in **Figure 15b**, the "Paraloid" here provides a good basis for the bonding of the AE sensors.

http://dx.doi.org/10.5772/63093

Figure 15. (a) "Paraloid" position with Japanese films and (b) bonding of the sensors.

The sensors have been arranged in positions useful to monitor simultaneously both the progress of the lesion and the detachment of the plaster. The detailed locations of the sensors are shown in **Figure 16**.

Figure 16. Detailed sensor positions.

The AE signals were picked up by a transducer and preamplified and transformed into electric voltage. Unwanted noisy signals were then eliminated by filtering frequencies, such as the vibration caused by the mechanical instrumentation, which is normally lower than 40 kHz. The signals were therefore analyzed by a measuring system that counts the signals that exceed a certain set voltage threshold measured in volts.

PZT sensors are set on a frequency range between 50 and 400 kHz. The data acquisition system consisted of six data storage provided trigger, six preamplified sensors, a central unit for the synchronization phase, and a threshold detector. From this monitoring system, microcrack localization is performed and the safe condition of the monitored specimen can be determined.

3.3. Results of the process based on the monitoring data

The monitoring work begun on 15:00 of April 28, 2011, and was planned to last for 6 months. In this part, only the monitoring data until 12:00 of June 4, 2011, were studied.

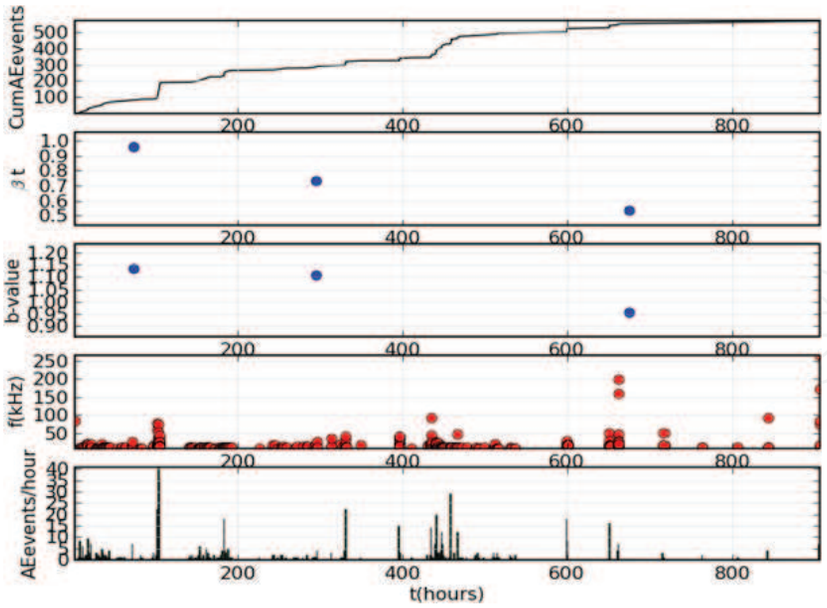

Figure 17. Results expression of sensors 1 to 4 near the lesion region.

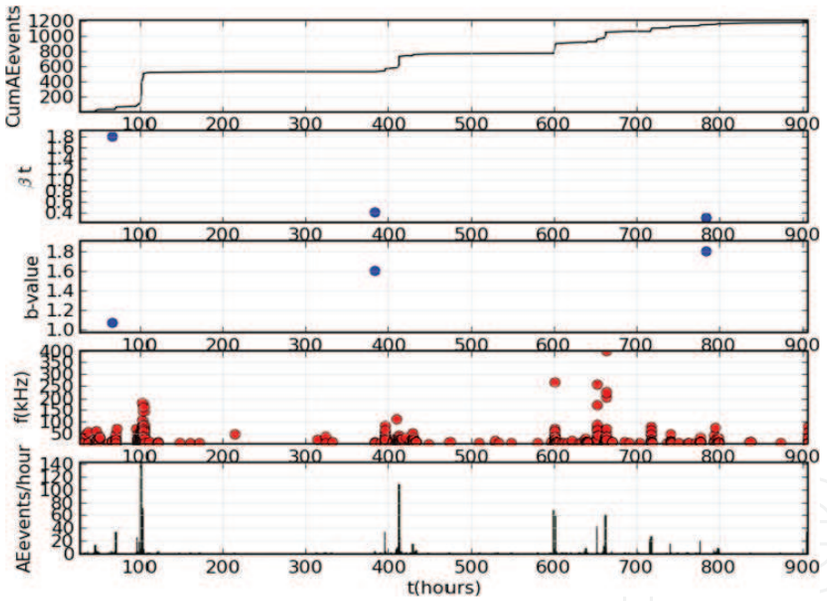

Figure 18. Results expression of sensors 5 and 6 near the detachment of the plaster.

Based on the monitoring data, the qualitative analysis of the data is mainly based on five techniques: the cumulative events analysis, the time dependence analysis, the *b*-value analysis, the amplitude of frequency analysis, and the event occurrence rate analysis. The results are shown in **Figures 17** and **18**. Considering the lesion condition in **Figure 17**, $0.5<b<1.0$ and $1.10<b<1.30$, both in average values of the three calculated points, means that the lesion region appears stable during the monitoring period and there are only some microcracks that happened. However, if we check the detachment condition of the plaster, $0.5<b<1.8$ and

http://dx.doi.org/10.5772/63093

1.10<*b*<1.80 show that a high-frequency event happens in this monitoring region and the detachment phenomena sometimes even occur during the monitoring period.

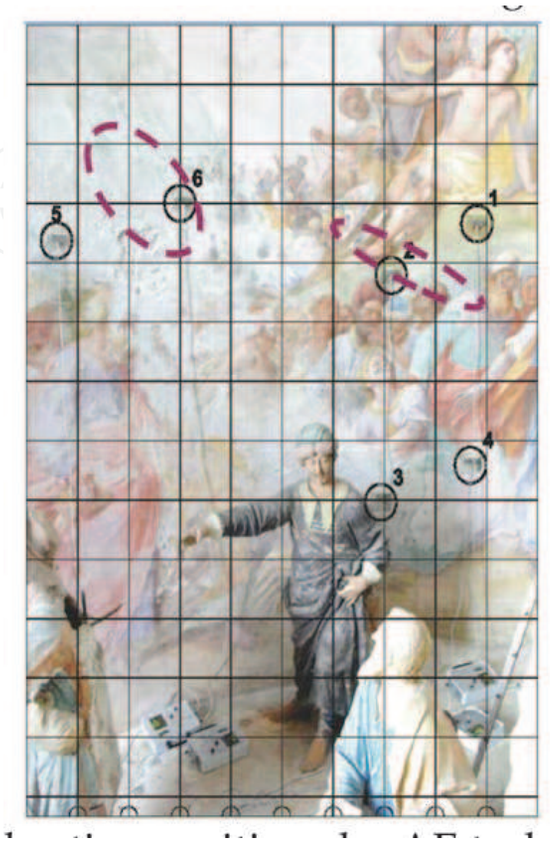

Figure 19. Monitored active positions by AE techniques are labeled by dashed lines.

According to the above qualitative analysis of the monitoring results, we know that the lesion region of the Chapel XVII appears to be stable during the monitoring period with some microcrack occurrence. As shown in **Figure 19**, the region around sensor 2 should be a more active region for lesion, and we should pay more attention on this region. On the contrary, the condition is not so good for the detachment area and the detachment phenomenon occurs with high frequency, especially for the region around sensor 6, as shown in **Figure 19**. Some maintenance measures should be implemented on this region.

4. Discussion and conclusions

Due to the increasing demand of structural retrofit and strengthening, monitoring techniques have received high attention. AE is one of the nondestructive monitoring techniques, which is widely employed for the cracking analysis in steel and concrete structures. However, the application of AE techniques to monitor masonry structures is complicated due to the fact that attenuation and wave propagation are highly dependent on the heterogeneity of the material.

Based on this problem, quantitative and qualitative analyses were proposed in this research to make the AE monitoring in masonry possible and reliable.

Crack localization is an important function in the quantitative analysis to offer the information of the active damage region. Considering the complicated material properties of masonry making the traditional localization method cannot be used directly, one modified method was proposed in this research. The proposed modified method of localization permits giving reasonable location results. In the proposed modified method, a modified factor k_i related to inhomogeneous or propagation delay is employed. The degree of heterogeneity ξ in k_i plays an important role to minimize the effect of the inhomogeneous of the material. The value ξ can be obtained by the pencil-lead break velocity field tests on the masonry structure and employed in the monitoring process. The ad hoc test results have shown that the results by the proposed modified method of localization are all located around the real crack positions. This proves that the proposed method can be a reliable and suitable one compared to the traditional one.

Besides the quantitative analysis, the qualitative analysis can also be used to monitor masonry structures. The application of the qualitative analysis was explained by monitoring one historical chapel. The cumulative events analysis, the time dependence analysis, the *b*-value analysis, the amplitude of frequency analysis, and the event occurrence rate analysis were adopted to analyze the stability of the monitoring areas.

In conclusion, quantitative and qualitative analyses proposed in this research can help to make good use of the AE technique to monitor masonry structures, and sometimes, better results can be driven if the two analysis methods can be used simultaneously.

Author details

Jie Xu*, Qinghua Han and Ying Xu

*Address all correspondence to: jxu@tju.edu.cn

School of Civil Engineering, Key Laboratory of Coast Civil Structure Safety, Tianjin University, Ministry of Education, 92 Weijin Rd, Nankai, Tianjin, China

References

[1] Dutta D, Sohn H, Harries KA, Rizzo P. A nonlinear acoustic technique for crack detection in metallic structures. Structural Health Monitoring. 2009;8(3):251–262.

[2] McCabe W, Koerner RM, Load AE. Acoustic emission behavior of concrete laboratory specimens. Journal of the American Concrete Institute. 1976;13:367–371.

[3] Köppel S, Vogel T. Localization and identification of cracking mechanisms in reinforced concrete using acoustic emission analysis. In: Proceedings of the Fourth International Conference on Bridge Management; Surrey. 2000.

[4] Carpinteri A, Lacidogna G, Niccolini G, Puzzi S. Critical defect size distributions in concrete structures detected by the acoustic emission technique. Meccanica. 2008;43:349–363.

[5] Holford KM, Pullin R, Lark RJ. Acoustic emission monitoring of concrete hinge joint models. In: Proceedings of the 26th European Conference on Acoustic Emission Testing; Berlin. 2004.

[6] Lovejoy SC. Development of acoustic emissions testing procedures applicable to conventionally reinforced concrete deck girder bridges subject tension cracking [thesis]. Oregon State University, Corvallis. 2006.

[7] Ohtsu M, Uchida M, Okamoto T, Yuyama S. Damage assessment of reinforced concrete beams qualified by acoustic emission. ACI Structural Journal. 2002;99(4):411–418.

[8] Carpinteri A, Lacidogna G. Damage diagnosis in concrete and masonry structures by acoustic emission technique. Facta Universitatis. 2003;3:755–764.

[9] Cullington DW, MacNeil D, Elliott J. Continuous acoustic monitoring of grouted post-tensioned concrete bridges. NDT & E International. 2001;34(2):95–105

[10] Giurgiutiu V, Zagrai, A, Bao JJ. Piezoelectric wafer embedded active sensors for aging aircraft structural health monitoring. Structural Health Monitoring. 2002;1(1):41–61.

[11] Golaski L, Gebski P, Ono K. Diagnostics of reinforced concrete bridges by acoustic emission. Journal of Acoustic Emission. 2002;2:83–98.

[12] Chang PC, Flatau A, Liu SC. Review paper: Health monitoring of civil infrastructure. Structural Health Monitoring. 2003;2(3):257–267.

[13] Carpinteri A, Invernizzi S, Lacidogna G. Structural assessment of a XVIIth century masonry vault with AE and numerical techniques. International Journal of Architectural Heritage. 2007;2:214–226.

[14] Melbourne C, Tomor AK. Application of acoustic emission for masonry arch bridges. Strain. 2006;42:165–172.

[15] Verstrynge E, Schueremans L, Gemert DV, Wevers M. Application of the acoustic emission technique to assess damage in masonry under increasing and sustained axial loading. In: NDTCE'09, Non-Destructive Testing in Civil Engineering; Nantes, France. 2009.

[16] Carpinteri A, Lacidogna G, Manuello A, Binda L. Monitoring the structures of the ancient temple of Athena incorporated into the cathedral of Syracuse. In: Proceedings of the 14th International Brick and Block Masonry Conference; Sydney, Australia. 2008.

[17] Tomor AK, Melbourne C. Monitoring masonry arch bridge response to traffic loading using acoustic emission techniques. In: Proceedings of the 5th International Conference on Arch Bridges; Madeira, Portugal. 2007.

[18] Ge M. Analysis of source location algorithms, part I: Overview and non-iterative methods. Journal of Acoustic Emission. 2003;21:14–28.

[19] Han QH, Xu J, Carpinteri A, Lacidogna G. Localization of acoustic emission sources in structural health monitoring of a masonry bridge. Structural Control and Health Monitoring. 2015;22(2):314–329.